Hindawi
International Journal of Biomaterials
Volume 2022, Article ID 6859637, 12 pages
https://doi.org/10.1155/2022/6859637

Research Article

Optimization, Characterization, and Anticancer Potential of Silver Nanoparticles Biosynthesized Using *Olea europaea*

Afnan I. Felimban,[1] **Njud S. Alharbi**,[1] **and Nehad S. Alsubhi**[2]

[1]*Department of Biological Sciences, Faculty of Science, King Abdulaziz University, Jeddah 21589, Saudi Arabia*
[2]*Department of Biological Science, Faculty of Science, University of Jeddah, Jeddah, Saudi Arabia*

Correspondence should be addressed to Afnan I. Felimban; aifelimban@stu.kau.edu.sa

Received 2 August 2022; Accepted 15 September 2022; Published 26 September 2022

Academic Editor: Sameh Ali

Green synthesis has attracted significant attention as an eco-friendly, low-cost, energy-efficient, and non-toxic method for preparing silver nanoparticles (AgNPs) for cancer therapy. This study optimized the green synthesis of AgNPs using *Olea europaea* extracts and evaluated their anticancer potential. The biosynthesized AgNPs were characterized using various methods, showing stable AgNPs with a desirable morphology and high yield, improving the properties of AgNPs for various medicinal applications. The biosynthesized AgNPs were predominantly spherical, with small sizes ranging from 13 to 21 nm and highly stable at −23 and −24 mV. The findings of this study suggest that green-synthesized AgNPs using *Olea europaea* and sunlight possess significant anticancer activity against cancer cells *in vitro*. Further investigation of green synthesis would help to form high-quality AgNPs that have promising potential in treating disease and fighting undesirable pathogens.

1. Introduction

Nanotechnology is a scientific field that involves the creation and application of nanosized particles. Nanoparticles are well-known as particles that range between 1 nm and 100 nm in diameter. The physical, chemical, and biological properties of these particles can be easily modified and used in various applications [1]. Therefore, they have attracted intensive studies in different fields, such as biology, chemistry, agriculture, and electronics [2]. Consequently, these small particles have a positive impact on food production, pharmaceuticals, and drug and gene delivery [3, 4].

Nanoparticles can be classified into several types based on their morphology and physical and chemical properties. Metal nanoparticles such as gold, silver, zinc, and iron can be made of pure metals or compounds. Among the metal nanoparticle types, silver nanoparticles (AgNPs) are the most important. AgNPs have numerous applications in different fields because of their unique properties [5–7].

Top-down and bottom-up methods are the two major approaches for synthesizing nanoparticles [8]. The top-down approach involves breaking down bulk material structures into nanosized particles. Top-down methods offer high controllability of pattern size and shape while typically incurring high costs. In contrast, the bottom-up approach involves building nanomaterials from smaller entities. Bottom-up methods offer advantages such as low cost and productivity, while the lack of control over precision in particle shape and size is their biggest drawback. Sol-Gel and green synthesis are considered bottom-up methods [9].

Green synthesis is an easy way to obtain nanoparticles with more advantages than disadvantages. Green synthesis provides a fast, economical, nontoxic, eco-friendly, and biocompatible alternative to physical and chemical techniques [10]. The synthesis of AgNPs from plants offers many advantages such as easy processing, cost efficiency, and no culture requirement [11]. Phytochemicals in plants, such as polyphenols, flavonoids, tannins, proteins, and sugars, are responsible for synthesizing nanoparticles and serve as reducing and stabilizing agents. In addition to their powerful reduction properties, they can reduce Ag^+ into Ag^0. Furthermore, they serve as capping agents for the coating of

nanoparticles, providing greater stability in the size and shape of nanoparticles [12].

Reaction conditions, such as extract concentration, temperature, pH, and light intensity, can influence the production, characterization, and application of AgNPs [13]. Optimization of the reaction conditions can help produce nanoparticles with well-defined sizes and morphologies, thereby improving their properties [14, 15].

The present study optimized the green synthesis of AgNPs using *Olea europaea* extracts for improved biological applications. The fundamental aim of the study was to provide an alternative to physical and chemical techniques for producing high-quality AgNPs that would improve their biological efficacy without introducing hazardous chemicals. The aim included examining the antitumor activities of the biosynthesized AgNPs against breast cancer cells, achieving remarkable results.

2. Materials and Methods

The green synthesis of AgNPs using *O. europaea* extracts along with phytochemical screening, optimization, characterization, and anticancer activity evaluation is illustrated in the schematic diagram (Figure 1).

2.1. Plant Collection and Aqueous Extracts Preparation. Fresh *O. europaea* plants (Figure 2) were collected from the Al-Jouf region, Saudi Arabia, by the Al-Jouf Agricultural Development Company. Aqueous extracts were determined following the method described in a previous study [16]. The collected plant materials were washed individually with tap water and then washed several times with distilled water to remove contaminants. The washed plant materials were left to dry completely in the shade at 24°C. The dried leaves were then grounded into a fine powder, and the fruit slices were stored in airtight containers. For aqueous extraction, five grams of the fine powder were mixed with deionized water, and the mixture was boiled and then filtered through a coffee filter and Whatman No. 1 filter paper. The extracts were stored in a bottle at −4°C for further use.

2.2. Phytochemical Screening. The phytochemicals in the *O. europaea* extracts were identified using the standard procedures described in Table 1. These are as reported in previous studies, [17–19]. Phytochemicals are involved in the reduction and coating of AgNPs.

2.3. Optimization of Green Synthesis of AgNPs. Processing parameters, such as extract concentration, temperature, pH, and light intensity, were optimized to improve the quality of the AgNPs. The optimum AgNPs conditions were determined using the parameters with the best results to obtain the best possible production and quality of AgNPs. The primary synthesis of AgNPs was performed following the procedure described in a previous study [24]. An amount of aqueous plant solution was added to 1 mM of $AgNO_3$ solution at a specific ratio, and the green synthesis was monitored at various time intervals. The reduction of the silver ions into AgNPs was followed by a colour change of the solution from light to reddish-brown depending on the parameters studied, the change in colour confirmed the reduction. It is well-known that AgNPs exhibit a dark brownish colour in an aqueous solution owing to the excitation of the surface plasmon vibrations in the metal nanoparticles [25, 26]. Also, the results indicated that the phytochemicals of O. europaea extracts successfully reduced Ag + to silver nanoparticles in an aqueous solution. Under direct sunlight, the reaction led to rapid nanoparticle formation, possibly because the photons from sunlight accelerated the reaction [27]. It was also reported that a long-lasting dark brown colour confirmed that all silver ion has completely reduced into AgNPs [28]. The AgNPs solutions were then centrifuged at 10,000 RPM for 10 min; the centrifugation process was repeated three times. Finally, the purified AgNPs were collected to analyse their characteristics.

2.4. Characterization Techniques. The biosynthesized AgNPs were characterized using ultraviolet-visible spectroscopy (UV-Vis), Fourier-transform infrared (FTIR) spectroscopy, dynamic light scattering (DLS), zeta potential analysis, and field-emission scanning electron microscopy (FE-SEM). For illustration, the green synthesis of AgNPs was monitored using a Cary® 50 ultraviolet-visible spectrophotometer in the 300–600 nm wavelength range. The association of biomolecules involved in the formation and stabilization of AgNPs were detected using an FTIR spectrometer (Fisher Nicolet iS10) in the 600–4000 cm^{-1} wavelength range. The particle hydrodynamic size distribution and stability of the AgNPs were observed using DLS and zeta potential using a Zetasizer Nano (Malvern Instruments Ltd., U.K.). The morphology, size, and shape of biosynthesized AgNPs are considered essential characteristics of nanoparticle systems because they determine their biological activity and toxicity [29]. Thus, they were analysed using field-emission scanning electron microscopy (JEO, JSM 7600F).

2.5. Cell Lines and Cell Cultures. The human hormone-dependent breast cancer cell lines, MCF7 and T47D, were obtained from the King Fahd Medical Research Centre. The cells were maintained in a high-glucose Dulbecco's Modified Eagle Medium (DMEM), supplemented with 10% fetal bovine serum (FBS) and 1% penicillin-streptomycin (Beijing Solarbio Science and Technology Co., Ltd., China). Cancer cells were grown in a humidified 5% CO_2 incubator at 37°C and passaged three times per week.

2.6. In Vitro Assay for Cytotoxicity Activity (MTT Assay) Anticancer Activity. The cytotoxicity of green-synthesized AgNPs dissolved in 0.3 dimethyl sulfoxide DMSO (AgNPs), *O. europaea* leaf extract (OLE) and AgNPs dissolved in leaf extract (AgNPs-OLE) samples were evaluated using the MTT assay. An MTT assay was performed according to the method described in a previous study [30]. Cells were seeded

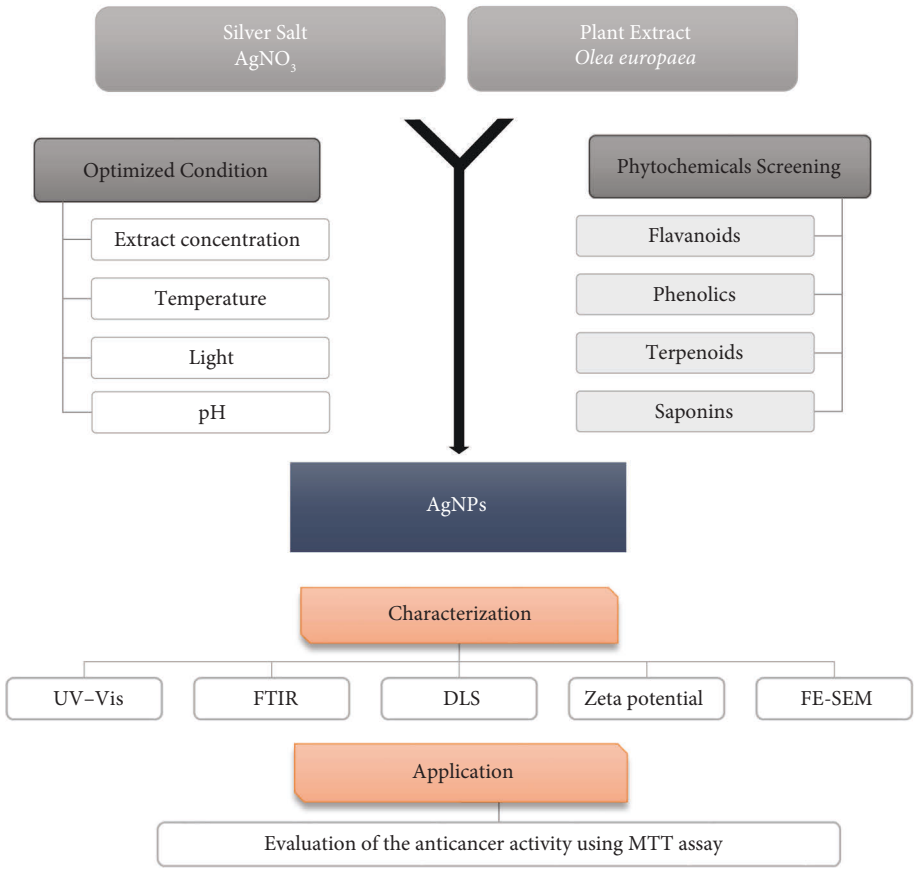

FIGURE 1: Schematic diagram of the green synthesis of silver nanoparticles (AgNPs) using *Olea europaea* extracts: phytochemical screening, optimization, characterization, and anticancer activity evaluation.

Olea Europaea Leaf *Olea Europaea* Fruit

FIGURE 2: *Olea europaea* leaves and fruit.

at a concentration of 1×10^4 cells per well in 96 well plates supplied with DMEM. The plates were incubated for 24 h at 37°C and maintained in a 5% CO^2 atmosphere to allow the cells to adhere overnight. Thereafter, the cells were treated with different concentrations (25, 50, 100, 150, and 200 μg/mL) of treatments in triplicate and incubated for 24 h, and the control cell cultures were left untreated. After incubation, the old media was discarded, and 100 μL of MTT solution was added to each well. The 96 well plates were then incubated for approximately 3–4 h until formazan crystals formed. The medium was then replaced with a 100 μL of DMSO solution and the OD was measured using an ELISA

Table 1: Phytochemical analysis of *Olea europaea* extracts standard procedures.

Phytochemicals	Tests	References
Phenolic	**Ferric chloride test:** a few drops (3–4 drops) of ferric chloride solution were added to 1 ml of the plant extract. The formation of bluish black confirms the presence of phenols.	[20]
Flavonoids	**Lead acetate test:** a few drops of 10% dilute lead acetate solution were added to the plant extract. The formation of the yellow precipitate confirms the presence of flavonoids.	[21]
Terpenoids	**Liebermann–Burchard test:** a few drops of sulphuric acid were added to 1 ml of the plant extract, and the formation of a brown ring at the junction and red colour in the upper layer confirms the presence of terpenoids.	[22]
Saponins	**Frothing test:** plant extract was treated with distilled water in a tube and shaken well. The formation of stable froth confirms the presence of saponins.	[23]

reader at 570 nm. The cytotoxic effects of the three treatments on breast cancer cells were expressed as the % cell viability using the following formula:

$$\%\text{cell viability} = \frac{\text{Absorbance treated cells} - \text{Absorbance blank}}{\text{Absorbance control cells} - \text{Absorbance blank}} \times 100. \quad (1)$$

(i) Blank refers to the background, which means the medium, MTT solution, and DMSO.

(ii) Control cells refer to untreated cells.

2.7. Statistical Analyses. Statistical analyses were performed using SPSS software. All data were analysed using one-way analysis of variance (ANOVA) followed by Tukey's post hoc test for multiple comparisons, and significance was considered $P < 0.05$.

3. Results and Discussion

3.1. Phytochemical Screening Analysis. Phytochemical screening analysis confirmed the presence of flavonoids, phenols, triterpenes, and saponins in the *O. europaea* extracts, as listed in Table 2. These phytochemicals play an essential role in the bio-reduction of Ag^+ to Ag^0 and the stabilization of biosynthesized AgNPs.

3.2. Optimization of the Green Synthesis Using UV-Vis Spectroscopy Analysis

3.2.1. Effect of Extract Concentration. To examine the effect of the extract concentration, three different volumes of 1, 2, and 3 mL of each extract were added separately to 9 mL of 1 mM $AgNO_3$ solution. Thus, reaction mixtures with the ratios of 1 : 9, 2 : 9, and 3 : 9 plant extract to 1 mM $AgNO_3$ silver nitrate were prepared, following the process described in an earlier study [31]. Increasing the plant extract volume in the reaction mixture increased the productivity of AgNPs, as shown in Figure 3(a). The plasmon resonance band in the 3 : 9 ratio sample was higher and appeared at a wavelength of 449 nm for the olive leaf and 464 nm for the olive fruit extract. Increasing the extract concentration increases the biomolecule content, resulting in a more intense colour. This finding is consistent with that reported in previous research [32]. Biomolecules act as reducing and capping agents at higher extract concentrations, protecting the synthesized nanoparticles from aggregation and affecting their size.

Table 2: Phytochemical screening test results of *Olea europaea* extracts.

Tested phytochemicals	*Olea europaea leaf*	*Olea europaea* fruit
Phenolic	+	+
Flavonoids	+	+
Terpenoids	+	+
Saponins	+	–

+ presence and – absence.

3.2.2. Effect of Temperature. The biosynthesized AgNPs were prepared at different reaction temperatures (40, 60, and 80°C), following the method of a previous study [33]. The results show an increase in the formation rate of AgNPs with increasing reaction temperature, as illustrated in Figure 3(b). The results also showed that the UV spectral wavelength decreased as the temperature increased, reducing the size of the AgNPs due to the rapid consumption of reactants. Higher temperatures resulted in higher rates of AgNPs formation. This is attributed to the fact that silver ions are consumed faster, leaving fewer opportunities for nanoparticles to grow. This finding is consistent with findings in an earlier study [34], confirming that increasing the temperature can increase the absorbance intensity at which small-sized AgNPs form rapidly. Another study [35] found the same results, confirming that increasing temperature can rapidly form AgNPs, directly affecting the nanoparticle size and shape.

3.2.3. Effect of pH. The effect of pH on the synthesis process was investigated at three different pH values: acidic (pH = 4), neutral (pH = 7), and basic (pH = 9). The pH of the green synthesis mixture was adjusted to the desired value using 0.1 N sodium hydroxide and 0.5 N acetic acid. Figure 4(c) shows the UV-vis absorption spectra of the AgNPs synthesized at three different pH values. The results showed that the highest reaction rate was observed at a pH of 9. The results show that an alkaline pH can promote the reaction of synthesized AgNPs, confirming the results reported in a previous investigation [36]. These results suggest that the efficient production of small AgNPs could be due to a large number of functional groups available for Ag binding under higher pH conditions, as earlier reported [37]. For illustration, the primary influence of the reaction pH is its ability to change the electrical charges of biomolecules, which may

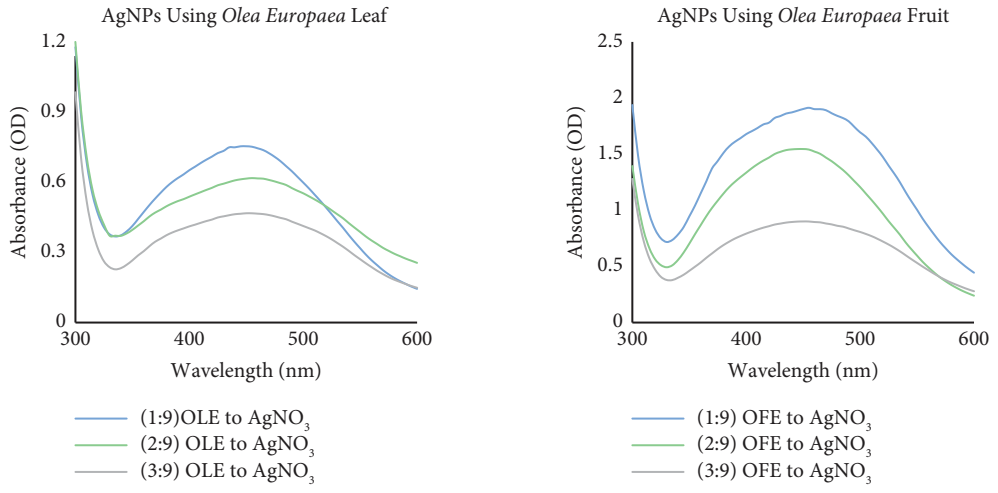

(a)

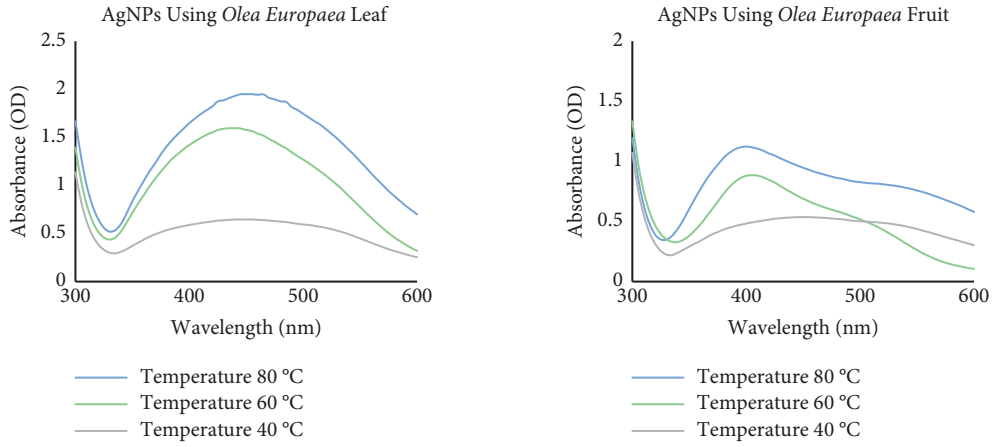

(b)

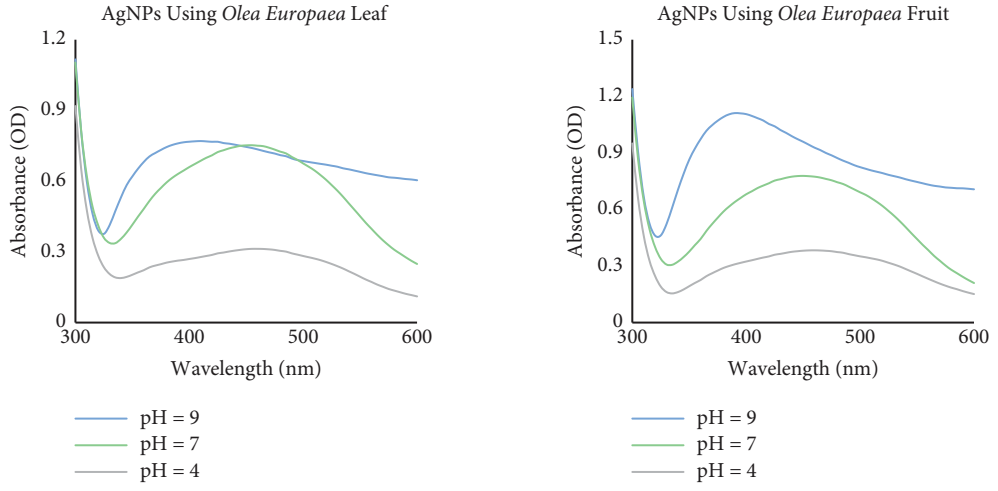

(c)

Figure 3: Continued.

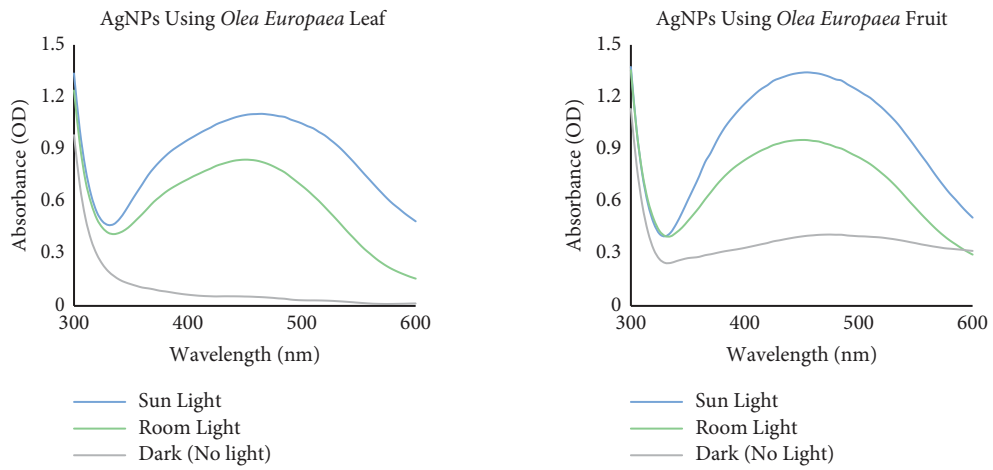

Figure 3: UV-vis absorption spectra of AgNPs synthesized using *Olea europaea* extracts at various operational parameters: (a) extract concentration using different ratios of plant extract to $AgNO_3$, (b) temperature, (c) change in pH, and (d) change in light intensities.

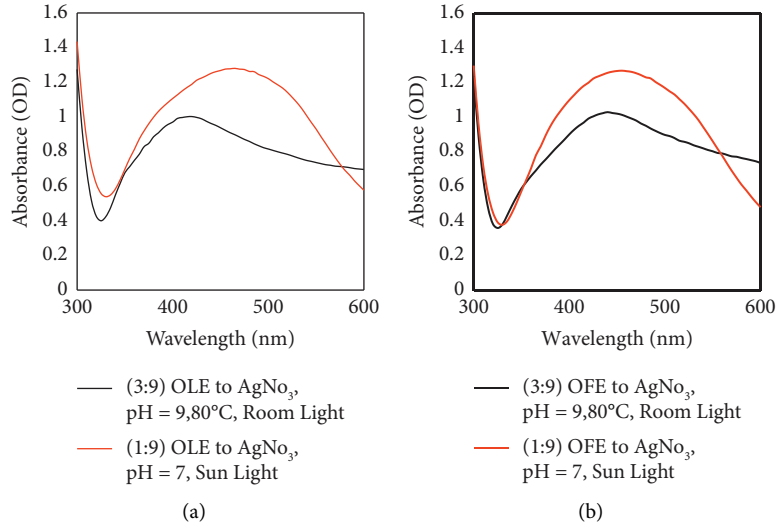

Figure 4: UV-vis absorption spectra of AgNPs synthesized using *Olea europaea* (a) leaf extract and (b) fruit extract at optimum production conditions in the current study for green synthesis of AgNPs.

affect their capping and stabilizing properties and, subsequently, the growth of the synthesized AgNPs [38]. The alkaline pH allows more hydroxyl (O-H) groups of plant extracts to participate in the reduction reaction, improving the yield of the green synthesis [39]. The results, therefore, showed that the nanoparticle size decreased with the increasing pH with lower aggregation, thus increasing particle stability. Similar findings have been reported in a previous investigation. A previous study reported that the AgNPs synthesis rate increased as the pH increased to 7 and then decreased when the pH value increased further [40]. In contrast, the reduction was mainly accomplished at acidic pH through ionic bonding and biomolecules due to the positively charged functional groups. Thus, many biomolecules bind when synthesizing AgNPs, resulting in agglomeration and larger-sized AgNPs [41, 42]. Hence, adjusting the pH could help control the size and stability of the AgNPs.

3.2.4. Effect of Light. Light can considerably influence the green synthesis of AgNPs [43]. A spectral analysis of the samples grown under dark, room light, and sunlight conditions was performed using a UV-vis spectrophotometer [44]. The results in Figure 4(d) show the significant impact of light intensity on the absorbance patterns. Sunlight can help achieve the best formation rate of AgNPs. Under the sunlight condition, the plasmon absorption band was the highest. The UV-vis spectra showed maximum absorbance at a wavelength of 465 nm for olive leaf and 455 nm for olive fruit extract. However, no formation of AgNPs was observed under dark conditions after 24 h, and an insubstantial

amount of AgNPs was observed when olive fruit extract was used. These results suggest an increase in absorbance when the light intensity increases. A possible explanation might be that a more significant number of photons in direct sunlight can help catalyse the reducing process, significantly promoting the green synthesis of AgNPs, as previously reported [45].

After studying these parameters, two sets of working conditions were selected as the optimum reaction conditions to produce high-quality AgNPs. By examining the two sets, the set of 3 : 9 plant extract to $AgNO_3$, pH value of 9, temperature of 80°C, and room light produced a lower amount of AgNPs compared with 1 : 9 plant extract to $AgNO_3$, pH value of 7, and sunlight, as shown in Figure 4. Thus, the optimum conditions in the current study for the valuable, simple, and rapid green synthesis of AgNPs were 1 : 9 plant extract to $AgNO_3$, a pH value of 7, and sunlight, as shown in Figure 5. With the selected optimum production conditions, small AgNPs formed in a large amount within a few minutes, and they were simultaneously characterized by high stability. For example, using sunlight in the green synthesis of AgNPs can speed up the synthesis and still yield a high concentration of AgNPs characterized by good stability, as recorded in a previous investigation [46]. This result agrees with many previous studies that have reported an effective green synthesis of AgNPs using sunlight [47–49].

3.3. FTIR Analysis. An FTIR analysis helped identify the various biomolecules of the plant extracts responsible for capping and efficiently stabilizing the AgNPs. Figure 6(a) shows the FTIR absorption bands of *O. europaea* leaf extracts and biosynthesized AgNPs. The results showed a broad and robust peak at 3340.2 cm^{-1}, representing the hydroxyl (O-H) functional group and indicating the presence of a phenolic group. Additionally, the absorption peaks that emerged at 2962.2 and 1639.2 cm^{-1} correspond to the functional groups (C-H) and ($C = C$), respectively. In addition, the spectrum observed at 1064.5 cm^{-1} points to (C-O). Figure 6(b) displays several absorption peaks in the IR spectrum of *O. europaea* fruit extract and biosynthesized AgNPs. A broad peak, responsible for (O-H) stretching was seen at 3361.4 cm^{-1}. Characteristic peaks were also observed at 2954.5 (C-H), 1629.6 ($C = C$), and 1056.8 (C-O) cm^{-1}. The FTIR spectrum results confirmed that the bioactive compounds present in the plant extracts were adsorbed on the surface of the biosynthesis of AgNPs, which is in agreement with that reported in an earlier study [50]. The bio-compounds found in the tested *O. europaea* parts, phenolics, and flavonoids played an essential role in reducing, capping, and stabilizing the green-synthesized AgNPs, thus enhancing their properties [51, 52].

3.4. DLS and Zeta Potential. From the DLS analysis (Figure 7), the average hydrodynamic size of synthesized AgNPs using *O. europaea* leaf extract was found to be 182 nm with a single peak and a polydispersity index (PDI) of 0.2. In addition, the zeta potential was −24 mV with a sharp peak. However, the average hydrodynamic size, PDI, and zeta potential for synthesized AgNPs using *O. europaea* fruit extract were 66 nm, 0.2, and −23 mV, respectively. These numerical values for PDI are generally acceptable because the smaller the PDI, the more homogeneous nanoparticles are produced [37]. Zeta potentials of −23 and −24 mV (Figure 8) indicated a stable dispersion without notable AgNPs agglomeration over an extended time in the solution. Previous investigations have stated that nanoparticles with charges in the range of +30 mV to −30 mV are very stable, and those in the range of +15 mV to−25 mV are moderately stable [53–55].

3.5. FE-SEM Analysis. FE-SEM images helped visualize the morphology, shape, and size of the biosynthesized AgNPs. Figure 9 shows micrograph images of the biosynthesized AgNPs using O. europaea extracts. The FE-SEM revealed that the nanoparticles were predominantly spherical, with some aggregation. However, an agglomeration might be observed due to the high concentration during manual sample preparations. The size of the AgNPs varied between 13–21 nm for O. europaea leaves and between 14.9–23 nm for O. europaea fruit. Similar results were previously reported [56]. The size variation between the AgNPs synthesized using O. europaea leaves and fruit is due to the difference in the molecular make-up of the plant cell. The type and quantity of biomolecules and secondary metabolites in the cell affect the size and surface properties of the synthesized nanoparticles [57]. For illustration, the phytochemical components of the plant extract act as reducing and coating agents, influencing the size and stabilization of the nanoparticles. The robust coating of the synthesized nanoparticles can offer more stability, protecting against agglomeration and aggregation [58, 59].

After characterization of biosynthesized AgNPs, a better anticancer application would be obtained for AgNPs biosynthesized using *O. europaea* leaf rather than fruit because of their better stability, smaller size, and good shape.

3.6. Anticancer Activity Evaluation. The anticancer activities of AgNPs, OLE, and AgNPs-OLE were evaluated *in vitro* against T47D and MCF7 breast cancer cell lines, and their IC50 values were determined from a graph of cell viability measured over a range of concentrations between 25 and 200 μg/mL. The results showed that AgNPs, OLE, and AgNPs-OLE effectively inhibited the proliferation of T47D and MCF7 cancer cells in a dose-dependent manner after 24 h of treatment (Figure 10). The percentage of cell death in T47D and MCF7 cells gradually increased with the increasing concentrations of the three treatments. The cytotoxicity of the three treatments also revealed that their higher concentrations had significantly more toxic effects on the cell viability of both T47D and MCF7, suggesting that the AgNPs, OLE, and AgNPs-OLE mediated cell death in a concentration-dependent manner.

The IC50 values were 116 μg/mL for T47D cells in the presence of AgNPs, 176 μg/mL in the presence of OLE, and 84 μg/mL in the presence of AgNPs-OLE. The IC50 values obtained were less than 200 μg/mL. In contrast, the IC50 values of AgNPs, OLE, and AgNPs-OLE on MCF7 cells

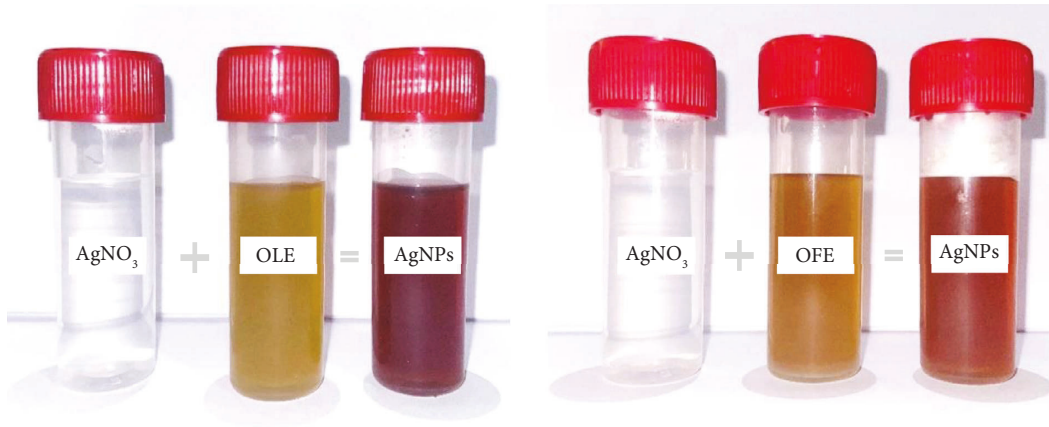

Figure 5: Visual observation of the green synthesis of silver nanoparticles (AgNPs) using *Olea europaea* leaf extract (OLE), and *Olea europaea* fruit extract (OFE).

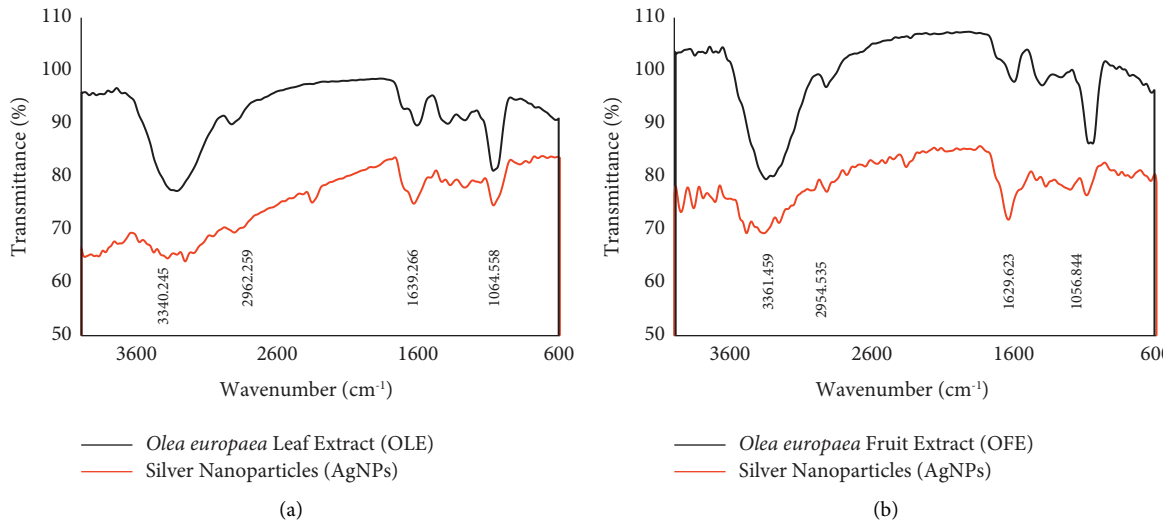

Figure 6: FTIR spectrum of plant extracts and AgNPs synthesized using *Olea europaea* (a) leaf extract and (b) fruit extract.

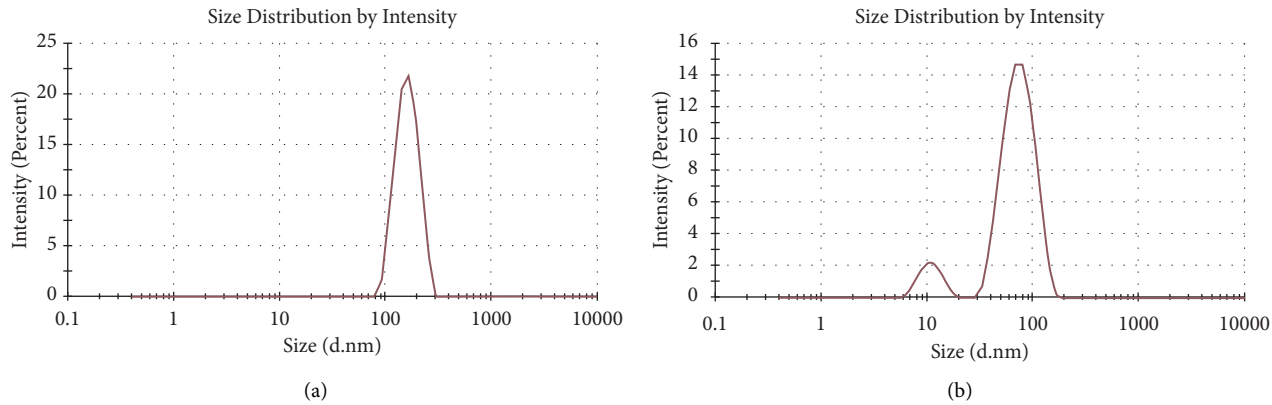

Figure 7: Particle size distribution of biosynthesized AgNPs using *Olea europaea* (a) leaf extract and (b) fruit extract.

were 80, 200, and 132 μg/mL, respectively. Thus, the results clearly demonstrated that the three treatments notably inhibited the cancer cells at moderate concentrations. Overall, the results of this study suggest that green-synthesized AgNPs possess significant anticancer activity in cancer cell lines.

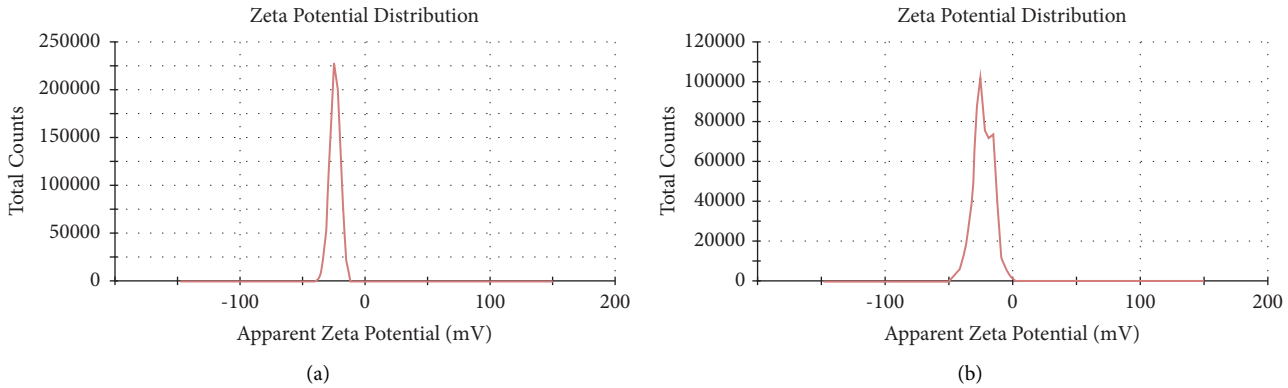

Figure 8: Zeta potential measurement of biosynthesized AgNPs using *Olea europaea* (a) leaf extract and (b) fruit extract.

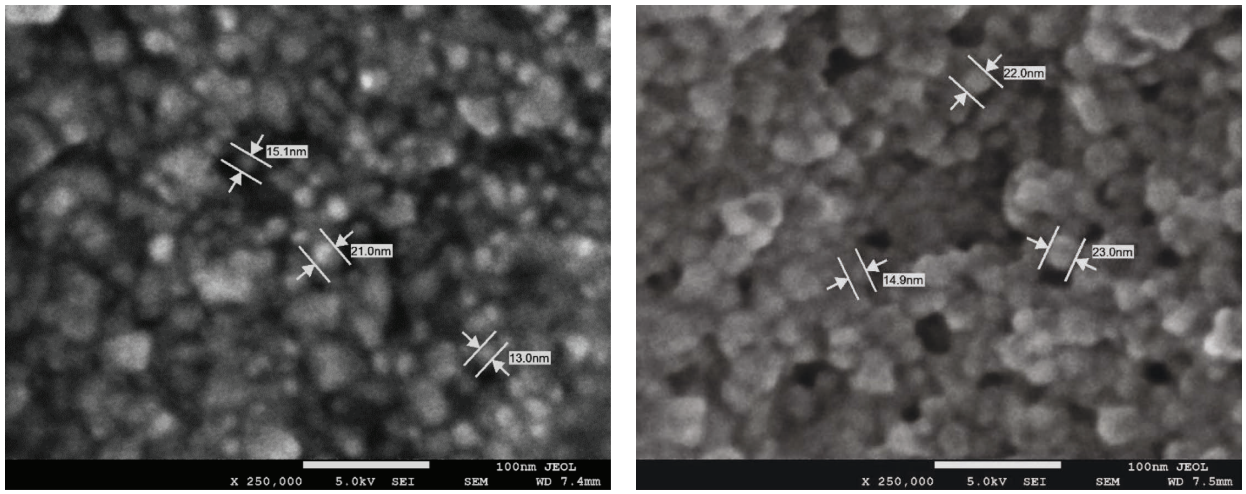

Figure 9: FE-SEM images of biosynthesized AgNPs using *Olea europaea* (a) leaf extract and (b) fruit extract.

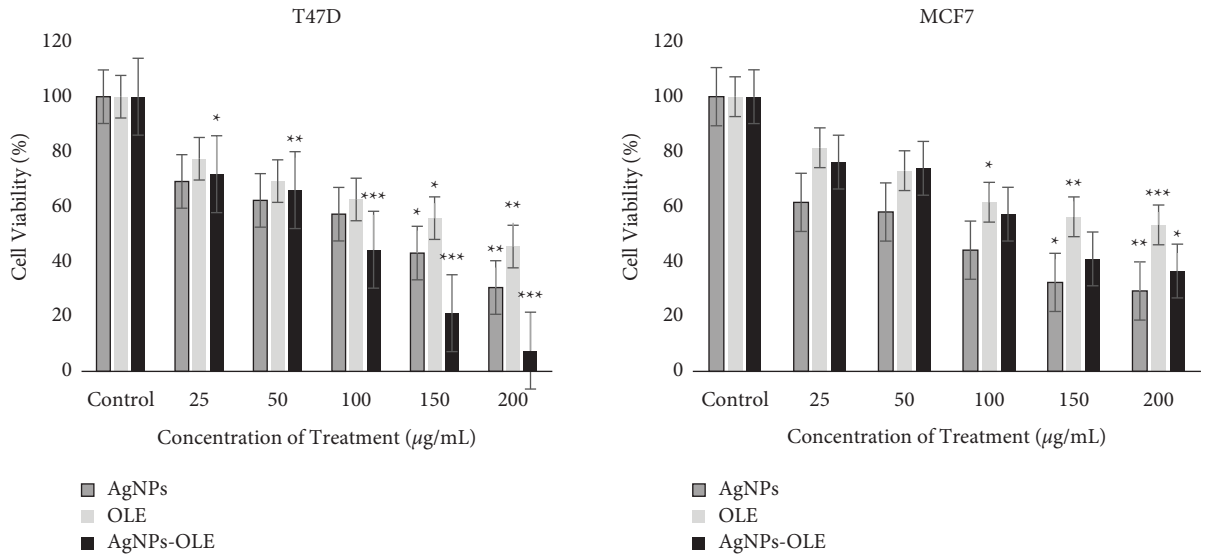

Figure 10: Cytotoxicity effects of AgNPs, OLE, and AgNPs-OLE on the viability of T47D and MCF7 after 24 h exposure. (Results are viable in comparison with the control (untreated cells). Data were analysed by applying one-way analysis of variance (ANOVA) with Tukey's posthoc tests; $^{*}P$ value <0.05, $^{**}P$ value <0.01, and $^{***}P$ value <0.001).

The higher efficacy of the synthesized AgNPs using O. europaea leaf extract against breast cancer cells might be due to their smaller size, which facilitates cell entry. The phytochemicals of O. europaea leaf extract enhanced the AgNPs biocompatibility and facilitated cellular access. A possible explanation for the results is that AgNPs perform as cancer therapeutics due to their potential ability to disrupt the mitochondrial respiratory chain, which induces the production of reactive oxygen species, causing DNA damage [60, 61].

Although a few previous studies considered the biosynthesis of AgNPs using O. europaea extracts [38, 40, 52], promoting AgNPs production using sunlight was not considered. The current study evaluated the effect of light intensity on the biosynthesized AgNPs using O. europaea, and a quick bio-reduction and small stable AgNPs with high yield were achieved using sunlight. We believe our study makes a significant contribution to the literature because, to our knowledge, this is the first inclusive study to apply green-synthesized AgNPs using O. europaea extract and sunlight to MCF7 and T47D cells. The findings presented provide convincing evidence of the promising biomedical and therapeutic applicability of AgNPs green-synthesized using O. europaea, which warrants further investigation and is clinically and academically relevant. However, this study had some limitations that need to be considered. With the variety and complexity present in the phytochemical composition of plant extracts, it is challenging to determine their full role in the reduction reactions and coating processes that control the size, shape, and stability of the nanoparticles [62]. Further, the type of solvent used is critical in the green synthesis of nanoparticles. The universal solvent, water, was chosen in this study as it is the safest, least expensive, and most eco-friendly solvent. Moreover, factors such as agglomeration and aggregation should be studied extensively, as they influence the efficiency of AgNPs applications [63, 64]. Another limitation of this study is that only in vitro experiments were conducted, and in vivo experiments would be necessary for the future clinical translation of the results.

4. Conclusion

Green synthesis of AgNPs using *O. europaea* extracts was performed, and AgNPs with well-defined morphologies were created. The results showed that the reaction parameters had substantial effects on the green synthesis of the AgNPs. Based on the results of the current study, the valuable, simple, and rapid formation of green-synthesized AgNPs can be achieved using sunlight. The FTIR analysis revealed the presence of some functional groups (O-H), (C-H), ($C = C$), and (C-O) and confirmed that the bio-compounds, phenolics, and flavonoids present in the plant extracts were adsorbed on the surface of the AgNPs, thus enhancing their properties and future applications. The different biosynthesized AgNPs were spherical and ranged in size between 13–21 nm for *O. europaea* leaf and between 14.9–23 nm for *O. europaea* fruit. Furthermore, the cytotoxicity results of green-synthesized AgNPs using *O. europaea* leaf extract, OLE, and AgNPs-OLE suggest that they possess significant anticancer activity against human breast cancer (T47D and MCF7) cell lines. These results prove that green synthesis of AgNPs via *O. europaea* extracts is an excellent way to create nanoparticles with well-defined sizes and morphologies, which could have various novel therapeutic applications.

This study focused on the green synthesis of AgNPs via medicinal plants as a fast, simple, economic, nontoxic, eco-friendly, and biocompatible technique. In addition, future optimization of the green synthesis conditions will help produce particles with well-defined sizes and morphologies, thereby improving the properties of the nanoparticles. This would enhance the widespread therapeutic application of AgNPs and would bring forward the investigation into toxicity and clinical research, offering good opportunities to fight several diseases and undesirable pathogens using nanotechnology with natural compounds, leading to new insights and new types of medicine.

Data Availability

The data used to support the findings of this study are included within the article, and necessary explanations in relation to this can be obtained from the corresponding author upon request.

Conflicts of Interest

The authors declare that they have no conflicts of interest.

Acknowledgments

This project was funded by the Deanship of Scientific Research (DSR), King Abdulaziz University, Jeddah, Saudi Arabia under grant no. (KEP-PHD-90-130-42). The authors, therefore, acknowledge with thanks DSR technical and financial support.

References

[1] R. Feynman, "There's plenty of room at the bottom" (original from 1995)," *Science*, vol. 254, p. 1300, 1991.

[2] I. Khan, K. Saeed, and I. Khan, "Nanoparticles: properties, applications and toxicities," *Arabian Journal of Chemistry*, vol. 12, no. 7, pp. 908–931, 2019.

[3] A. Azadpour, S. Hajrasouliha, and S. Khaleghi, "Green synthesized-silver nanoparticles coated with targeted chitosan nanoparticles for smart drug delivery," *Journal of Drug Delivery Science and Technology*, vol. 74, Article ID 103554, 2022.

[4] M. A. Robles-García, F. Rodríguez-Félix, E. Márquez-Ríos et al., "Applications of nanotechnology in the agriculture, food, and pharmaceuticals," *Journal of Nanoscience and Nanotechnology*, vol. 16, no. 8, pp. 8188–8207, 2016.

[5] F. Ö. Küp, S. Çoşkunçay, and F. Duman, "Biosynthesis of silver nanoparticles using leaf extract of Aesculus hippocastanum (horse chestnut): evaluation of their antibacterial, antioxidant and drug release system activities," *Materials Science and Engineering: C*, vol. 107, Article ID 110207, 2020.

[6] M. S. Mehata, Aryan, and M. S. Mehata, "Surface plasmon resonance allied applications of silver nanoflowers

synthesized from Breynia vitis-idaea leaf extract," *Dalton Transactions*, vol. 51, no. 7, pp. 2726–2736, 2022.

[7] D. H. Nguyen, J. S. Lee, K. D. Park et al., "Green silver nanoparticles formed by Phyllanthus urinaria, Pouzolzia zeylanica, and Scoparia dulcis leaf extracts and the antifungal activity," *Nanomaterials*, vol. 10, no. 3, p. 542, 2020.

[8] M. A. Meyers, A. Mishra, and D. J. Benson, "Mechanical properties of nanocrystalline materials," *Progress in Materials Science*, vol. 51, no. 4, pp. 427–556, 2006.

[9] H.-K. Chan and P. C. L. Kwok, "Production methods for nanodrug particles using the bottom-up approach," *Advanced Drug Delivery Reviews*, vol. 63, no. 6, pp. 406–416, 2011.

[10] M. Ovais, A. T. Khalil, M. Ayaz, I. Ahmad, S. K. Nethi, and S. Mukherjee, "Biosynthesis of metal nanoparticles via microbial enzymes: a mechanistic approach," *International Journal of Molecular Sciences*, vol. 19, no. 12, p. 4100, 2018.

[11] P. N. V. K. Pallela, S. Ummey, L. K. Ruddaraju, S. Pammi, and S.-G. Yoon, "Ultra Small, mono dispersed green synthesized silver nanoparticles using aqueous extract of Sida cordifolia plant and investigation of antibacterial activity," *Microbial Pathogenesis*, vol. 124, pp. 63–69, 2018.

[12] S. Bawazeer, A. Rauf, S. U. A. Shah et al., "Green synthesis of silver nanoparticles using Tropaeolum majus: phytochemical screening and antibacterial studies," *Green Processing and Synthesis*, vol. 10, no. 1, pp. 85–94, 2021.

[13] N. S. Alharbi, N. S. Alsubhi, and A. I. Felimban, "Green synthesis of silver nanoparticles using medicinal plants: characterization and application," *Journal of Radiation Research and Applied Sciences*, vol. 15, no. 3, pp. 109–124, 2022.

[14] R. H. Ahmed and D. E. Mustafa, "Green synthesis of silver nanoparticles mediated by traditionally used medicinal plants in Sudan," *International Nano Letters*, vol. 10, no. 1, pp. 1–14, 2020.

[15] A. A. Numan, M. Ahmed, M. S. A. Galil, M. Al-Qubati, A. A. Raweh, and E. A. Helmi, "Bio-Fabrication of silver nanoparticles using Catha edulis extract: procedure optimization and antimicrobial efficacy encountering antibiotic-resistant pathogens," *Advances in Nanoparticles*, vol. 11, no. 02, pp. 31–54, 2022.

[16] R. C. Fierascu, I. R. Bunghez, R. Somoghi, I. Fierascu, and R. M. Ion, "Characterization of silver nanoparticles obtained by using Rosmarinus officinalis extract and their antioxidant activity," *Revue Roumaine de Chimie*, vol. 59, no. 3-4, p. 213, 2014.

[17] A. Afreen, R. Ahmed, S. Mehboob et al., "Phytochemical-assisted biosynthesis of silver nanoparticles from Ajuga bracteosa for biomedical applications," *Materials Research Express*, vol. 7, no. 7, Article ID 075404, 2020.

[18] M. Arif, R. Ullah, M. Ahmad et al., "Green synthesis of silver nanoparticles using Euphorbia wallichii leaf extract: its antibacterial action against citrus canker causal agent and antioxidant potential," *Molecules*, vol. 27, no. 11, p. 3525, 2022.

[19] A. O. Dada, A. A. Inyinbor, E. I. Idu et al., "Effect of operational parameters, characterization and antibacterial studies of green synthesis of silver nanoparticles using Tithonia diversifolia," *PeerJ*, vol. 6, p. e5865, 2018.

[20] D. Kardong, S. Upadhyaya, and L. Saikia, "Screening of phytochemicals, antioxidant and antibacterial activity of crude extract of Pteridium aquilinum Kuhn," *Journal of Pharmacy Research*, vol. 6, no. 1, pp. 179–182, 2013.

[21] J. Harbone, *Phytochemical Methods: A Guide to Modern Techniques of Plant Analysis*, Charpman and Hall, London, UK, 3rd edition, 1973.

[22] A. Kumar, K. Jha, D. Kumar, A. Agrawal, and A. Gupta, "Preliminary phytochemical analysis of leaf and bark (mixture) extract of Ficus infectoria plant," *The Pharma Innovation*, vol. 1, no. 5, p. 71, 2012.

[23] M. Kavit, B. Patel, and B. Jain, "Phytochemical analysis of leaf extract of Phyllanthus fraternus," *Research Journal of Recent Sciences ISSN*, vol. 2277, p. 2502, 2013.

[24] S. Devanesan, M. S. Alsalhi, R. V. Balaji et al., "Antimicrobial and cytotoxicity effects of synthesized silver nanoparticles from punica granatum peel extract," *Nanoscale Res Lett*, vol. 13, no. 1, p. 315, 2018.

[25] P. Mulvaney, "Surface plasmon spectroscopy of nanosized metal particles," *Langmuir*, vol. 12, no. 3, pp. 788–800, 1996.

[26] K. Saware and A. Venkataraman, "Biosynthesis and characterization of stable silver nanoparticles using Ficus religiosa leaf extract: a mechanism perspective," *Journal of Cluster Science*, vol. 25, no. 4, pp. 1157–1171, 2014.

[27] M. Mankad, G. Patil, D. Patel, P. Patel, and A. Patel, "Comparative studies of sunlight mediated green synthesis of silver nanoparaticles from Azadirachta indica leaf extract and its antibacterial effect on Xanthomonas oryzae pv. oryzae," *Arabian Journal of Chemistry*, vol. 13, no. 1, pp. 2865–2872, 2020.

[28] G. Sharma, J. S. Nam, A. R. Sharma, and S. S. Lee, "Antimicrobial potential of silver nanoparticles synthesized using medicinal herb coptidis rhizome," *Molecules*, vol. 23, no. 9, p. 2268, 2018.

[29] S. F. Hashemi, N. Tasharrofi, and M. M. Saber, "Green synthesis of silver nanoparticles using Teucrium polium leaf extract and assessment of their antitumor effects against MNK45 human gastric cancer cell line," *Journal of Molecular Structure*, vol. 1208, Article ID 127889, 2020.

[30] T. Mosmann, "Rapid colorimetric assay for cellular growth and survival: application to proliferation and cytotoxicity assays," *Journal of Immunological Methods*, vol. 65, no. 1-2, pp. 55–63, 1983.

[31] S. Ahmed, Saifullah, M. Ahmad, M. Ahmad, B. L. Swami, and S. Ikram, "Green synthesis of silver nanoparticles using Azadirachta indica aqueous leaf extract," *Journal of Radiation Research and Applied Sciences*, vol. 9, no. 1, pp. 1–7, 2016.

[32] A. Verma and M. S. Mehata, "Controllable synthesis of silver nanoparticles using Neem leaves and their antimicrobial activity," *Journal of Radiation Research and Applied Sciences*, vol. 9, no. 1, pp. 109–115, 2016.

[33] O. Stavinskaya, I. Laguta, T. Fesenko, and M. Krumova, "Effect of temperature on green synthesis of silver nanoparticles using Vitex agnus-castus extract," *Chemistry Journal of Moldova*, vol. 14, no. 2, pp. 117–121, 2019.

[34] H. M. Ibrahim, "Green synthesis and characterization of silver nanoparticles using banana peel extract and their antimicrobial activity against representative microorganisms," *Journal of Radiation Research and Applied Sciences*, vol. 8, no. 3, pp. 265–275, 2015.

[35] M. Asimuddin, M. R. Shaik, S. F. Adil et al., "Azadirachta indica based biosynthesis of silver nanoparticles and evaluation of their antibacterial and cytotoxic effects," *Journal of King Saud University - Science*, vol. 32, no. 1, pp. 648–656, 2020.

[36] M. Riaz, V. Mutreja, S. Sareen et al., "Exceptional antibacterial and cytotoxic potency of monodisperse greener AgNPs prepared under optimized pH and temperature," *Scientific Reports*, vol. 11, no. 1, p. 2866, 2021.

[37] K. N. Nahar, M. Rahaman, G. Khan, M. Islam, and S. M. Al-Reza, "Green synthesis of silver nanoparticles from Citrus

sinensis peel extract and its antibacterial potential," *Asian Journal of Green Chemistry*, vol. 5, no. 1, p. 135, 2021.

[38] M. M. Khalil, E. H. Ismail, K. Z. El-Baghdady, and D. Mohamed, "Green synthesis of silver nanoparticles using olive leaf extract and its antibacterial activity," *Arabian Journal of Chemistry*, vol. 7, no. 6, pp. 1131–1139, 2014.

[39] M. Singh, I. Sinha, and R. K. Mandal, "Role of pH in the green synthesis of silver nanoparticles," *Materials Letters*, vol. 63, no. 3-4, pp. 425–427, 2009.

[40] M. Rashidipour and R. Heydari, "Biosynthesis of silver nanoparticles using extract of olive leaf: synthesis and in vitro cytotoxic effect on MCF-7 cells," *Journal of Nanostructure in Chemistry*, vol. 4, no. 3, p. 112, 2014.

[41] H. B. Habeeb Rahuman, R. Dhandapani, S. Narayanan et al., "Medicinal plants mediated the green synthesis of silver nanoparticles and their biomedical applications," *IET Nanobiotechnology*, vol. 16, no. 4, pp. 115–144, 2022.

[42] R. Veerasamy, T. Z. Xin, S. Gunasagaran et al., "Biosynthesis of silver nanoparticles using mangosteen leaf extract and evaluation of their antimicrobial activities," *Journal of Saudi Chemical Society*, vol. 15, no. 2, pp. 113–120, 2011.

[43] V. Rawat, A. Sharma, V. P. Bhatt, R. Pratap Singh, and I. K. Maurya, "Sunlight mediated green synthesis of silver nanoparticles using Polygonatum graminifolium leaf extract and their antibacterial activity," *Materials Today: Proceedings*, vol. 29, pp. 911–916, 2020.

[44] B. D. Lade and A. S. Patil, "Silver nano fabrication using leaf disc of Passiflora foetida Linn," *Applied Nanoscience*, vol. 7, no. 5, pp. 181–192, 2017.

[45] S. K. Srikar, D. D. Giri, D. B. Pal, P. K. Mishra, and S. N. Upadhyay, "Light induced green synthesis of silver nanoparticles using aqueous extract of Prunus amygdalus," *Green and Sustainable Chemistry*, vol. 06, no. 01, pp. 26–33, 2016.

[46] T. Prathna, N. Chandrasekaran, A. M. Raichur, and A. Mukherjee, "Biomimetic synthesis of silver nanoparticles by Citrus limon (lemon) aqueous extract and theoretical prediction of particle size," *Colloids and Surfaces B: Biointerfaces*, vol. 82, no. 1, pp. 152–159, 2011.

[47] V. Kumar, D. Bano, S. Mohan, D. K. Singh, and S. H. Hasan, "Sunlight-induced green synthesis of silver nanoparticles using aqueous leaf extract of Polyalthia longifolia and its antioxidant activity," *Materials Letters*, vol. 181, pp. 371–377, 2016.

[48] V. T. Nguyen, "Sunlight-driven synthesis of silver nanoparticles using pomelo peel extract and antibacterial testing," *Journal of Chemistry*, vol. 2020, Article ID 6407081, 9 pages, 2020.

[49] M. P. Sooraj, A. S. Nair, and D. Vineetha, "Sunlight-mediated green synthesis of silver nanoparticles using Sida retusa leaf extract and assessment of its antimicrobial and catalytic activities," *Chemical Papers*, vol. 75, no. 1, pp. 351–363, 2021.

[50] F. K. Alsammarraie, W. Wang, P. Zhou, A. Mustapha, and M. Lin, "Green synthesis of silver nanoparticles using turmeric extracts and investigation of their antibacterial activities," *Colloids and Surfaces B: Biointerfaces*, vol. 171, pp. 398–405, 2018.

[51] N. Raghavendra, L. V. Hublikar, S. M. Patil, and P. Bhat, "Microwave assisted biosynthesis of silver nanoparticles using banana leaves extract: phytochemical, spectral characterization, and anticancer activity studies," *Journal of Water and Environmental Nanotechnology*, vol. 6, no. 1, p. 49, 2021.

[52] H. Sellami, S. A. Khan, I. Ahmad, A. A. Alarfaj, A. H. Hirad, and A. E. Al-Sabri, "Green synthesis of silver nanoparticles using Olea europaea leaf extract for their enhanced antibacterial, antioxidant, cytotoxic and biocompatibility applications," *International Journal of Molecular Sciences*, vol. 22, no. 22, Article ID 12562, 2021.

[53] V. S. Kotakadi, S. A. Gaddam, S. K. Venkata, and D. V. R. Sai Gopal, "New generation of bactericidal silver nanoparticles against different antibiotic resistant *Escherichia coli* strains," *Applied Nanoscience*, vol. 5, no. 7, pp. 847–855, 2015.

[54] V. S. Kotakadi, S. A. Gaddam, S. K. Venkata, P. V. G. K. Sarma, and D. V. R. Sai Gopal, "Biofabrication and spectral characterization of silver nanoparticles and their cytotoxic studies on human CD34+ ve stem cells," *3 Biotech*, vol. 6, no. 2, p. 216, 2016.

[55] A. K. Suresh, M. J. Doktycz, W. Wang et al., "Monodispersed biocompatible silver sulfide nanoparticles: facile extracellular biosynthesis using the γ-proteobacterium, Shewanella oneidensis," *Acta Biomaterialia*, vol. 7, no. 12, pp. 4253–4258, 2011.

[56] A. Rautela, J. Rani, and M. Debnath Das, "Green synthesis of silver nanoparticles from Tectona grandis seeds extract: characterization and mechanism of antimicrobial action on different microorganisms," *Journal of Analytical Science and Technology*, vol. 10, no. 1, p. 5, 2019.

[57] H. Chugh, D. Sood, I. Chandra, V. Tomar, G. Dhawan, and R. Chandra, "Role of gold and silver nanoparticles in cancer nano-medicine," *Artificial Cells, Nanomedicine, and Biotechnology*, vol. 46, no. sup1, pp. 1210–1220, 2018.

[58] Z. E. Jiménez Pérez, R. Mathiyalagan, J. Markus et al., "Ginseng-berry-mediated gold and silver nanoparticle synthesis and evaluation of their in vitro antioxidant, antimicrobial, and cytotoxicity effects on human dermal fibroblast and murine melanoma skin cell lines," *International Journal of Nanomedicine*, vol. 12, pp. 709–723, 2017.

[59] D. Arumai Selvan, D. Mahendiran, R. Senthil Kumar, and A. Kalilur Rahiman, "Garlic, green tea and turmeric extracts-mediated green synthesis of silver nanoparticles: phytochemical, antioxidant and in vitro cytotoxicity studies," *Journal of Photochemistry and Photobiology B: Biology*, vol. 180, pp. 243–252, 2018.

[60] P. V. AshaRani, G. Low Kah Mun, M. P. Hande, and S. Valiyaveettil, "Cytotoxicity and genotoxicity of silver nanoparticles in human cells," *ACS Nano*, vol. 3, no. 2, pp. 279–290, 2009.

[61] K. S. Siddiqi, M. Rashid, A. Rahman, A. Husen, A. Husen, and S. Rehman, "Biogenic fabrication and characterization of silver nanoparticles using aqueous-ethanolic extract of lichen (Usnea longissima) and their antimicrobial activity," *Biomaterials Research*, vol. 22, no. 1, p. 23, 2018.

[62] A. Velidandi, S. Dahariya, N. P. P. Pabbathi, D. Kalivarathan, and R. R. Baadhe, "A review on synthesis, applications, toxicity, risk assessment and limitations of plant extracts synthesized silver nanoparticles," *NanoWorld Journal*, vol. 6, no. 3, p. 35, 2020.

[63] M. A. Ashraf, W. Peng, Y. Zare, and K. Y. Rhee, "Effects of size and aggregation/agglomeration of nanoparticles on the interfacial/interphase properties and tensile strength of polymer nanocomposites," *Nanoscale Research Letters*, vol. 13, no. 1, p. 214, 2018.

[64] T. Kavinkumar, K. Varunkumar, V. Ravikumar, and S. Manivannan, "Anticancer activity of graphene oxide-reduced graphene oxide-silver nanoparticle composites," *Journal of Colloid and Interface Science*, vol. 505, pp. 1125–1133, 2017.